Mutational analysis of the zinc and substrate binding sites in the CphA metallo-β-lactamase from Aeromonas hydrophila

Carine M Bebrone, Christine Anne, Frédéric Kerff, Gianpero Garau, Kris de Vriendt, Raphaël Lantin, Bart Devreese, Jozef van Beeumen, Otto Dideberg, J.-M. Frère, et al.

Mutational analysis of the zinc and substrate binding sites in the CphA metallo-β-lactamase from *Aeromonas hydrophila*

Carine Bebrone [*a], Christine Anne [*a], Frédéric Kerff [*], Gianpiero Garau[†], Kris De Vriendt[‡], Raphaël Lantin[*], Bart Devreese[‡], Jozef van Beeumen[‡], Otto Dideberg [†], Jean-Marie Frère [*] and Moreno Galleni [*]

[a] Both authors contributed equally to this work

[*] *Centre d'Ingénierie des Protéines, Université de Liège, Allée de 6 Août B6, Sart-Tilman 4000 Liège, Belgium*

[†] *Institut de Biologie Structurale Jean-Pierre Ebel (CNRS-CEA-UJF), rue Jules Horowitz 41, 38027 Grenoble Cedex 1, France*

[‡] *Laboratorium voor Eiwitbiochemie en Eiwitengineering, K.L. Ledeganckstraat 35, University of Gent, B-9000 Gent, Belgium*

Running Title: Zinc and substrate binding sites in CphA

Address correspondence to : Moreno Galleni, Macromolécules biologiques, Centre d'Ingénierie des Protéines, Université de Liège, Allée de 6 Août B6, Sart-Tilman 4000 Liège, Belgium; Fax. : 003243663364 ; E-mail : mgalleni@ulg.ac.be.

Abbreviations: EXAFS (Extended X-ray absorption fine structure), ICP-MS (inductively coupled plasma mass spectroscopy), PAC (perturbed angular correlation)

Synopsis

The subclass B2 CphA β-lactamase from *Aeromonas hydrophila* is a Zn(II) containing enzyme that hydrolyse specifically carbapenems. In an effort to evaluate residues potentially involved in metal binding and/or catalysis (His118, Asp120, His196 and His263) and in substrate specificity (Val67, Thr157, Lys224 and Lys226), site-directed mutants were generated and characterised.

Our results confirm that the first zinc ion is in interaction with Asp120 and His263, and thus is located in the "cysteine" zinc binding site. His118 and His196 residues seem to be in interaction with the second zinc ion as their replacement by alanine residues has a negative effect on the affinity for this second metal ion.

Val67 plays a significant role in the binding of biapenem and benzylpenicillin. The properties of a mutant with a five residues (LFKHV) insertion just after Val67 also reveal the importance of this region for substrate binding. This latter mutant has a higher affinity for the second zinc than the wild-type CphA. The T157A mutant exhibits a significant modification of the activity spectrum. The analysis of the K224Q and N116H-N220G-K224Q mutants points out a significant role for Lys224 in the binding of substrate. Lys226 is not essential for the binding and hydrolysis of substrates.

Thus, the present work helps to elucidate the position of the second zinc which was controversial and to identify residues important for substrate binding.

Keywords: β-lactamase, carbapenems, zinc binding sites, substrate binding, site-directed mutagenesis, enzymatic kinetics.

Introduction

In vivo, class B β-lactamases [1] require one or two zinc ions as enzymatic cofactors. By efficiently catalysing the hydrolysis of the β-lactam amide bond, these enzymes play a key role in bacterial resistance to this group of antibiotics. Several pathogens are now known to synthesize members of this class [2, 3, 4, 5, 6, 7]. Metallo-β-lactamases exhibit very broad activity spectra [8]. Moreover, they are not susceptible to the common β-lactamases inactivators [9]. No clinically efficient inhibitor of metallo-β-lactamases has been found yet. The fact that some of the metallo-β-lactamases genes are plasmid-encoded represents an additional cause of concern [10, 11]. On the basis of the known sequences, three different lineages, identified as subclasses B1, B2, and B3, can be characterized [12, 13]. The enzymes exhibit two potential zinc binding sites containing His(Asn)116, His118 and His196 in subclasses B1 and B3 (B2) and Asp120, Cys221 (His121) and His263 in subclasses B1 and B2 (B3). Each subclass thus possesses a different set of potential zinc ligands.

The CphA metallo-β-lactamase produced by *Aeromonas hydrophila* belongs to subclass B2 which is characterized by a uniquely narrow specificity profile. In contrast to metallo-β-lactamases of subclasses B1 and B3, CphA efficiently hydrolyses only carbapenems and shows very poor activity against penicillins and cephalosporins [8, 14] and exhibits a maximum activity as a mono-zinc enzyme. The presence of a Zn^{2+} ion in a second low affinity binding site noncompetitively inhibits the enzyme with a K_i value of 46 µM at pH 6.5 [15]. Recently, the structure of the mono-zinc CphA enzyme has been solved by X-ray cristallography [16]. Similarly to the known structures of metallo-β-lactamases of subclasses B1 [17-22] and B3 [23, 24], the X-ray structure of CphA highlights an αββα sandwich with two central β-sheets and α-helices on the external faces. The active site is located at the bottom of the β-sheet core. In contrast to all reported B1 and B3 subclass structures, a long α3 helix (Arg140-Leu161) is located near the active site groove of CphA. α3 is a key element of the "hydrophobic wall" which defines the active site pocket. Thus, whereas B1 and B3 enzymes exhibit a large cavity, the active site of CphA is very well defined and this explains the very narrow activity profile of the enzyme [16].

Contrary to the enzymes of subclasses B1 and B3, it was demonstrated that, in the subclass B2 CphA enzyme, a cysteine residue contributes to the first catalytic zinc

binding site [16, 25, 26, 27]. This result suggested that the respective binding sites of the first and second zinc ions would be reversed in CphA as compared to B1 and B3 metallo-β-lactamases. However, on the basis of spectroscopic studies with another subclass B2 enzyme (ImiS), Crawford and his co-workers [28, 29] postulate that the second zinc binding site is not the traditional "histidine" site, but involves both His118 and Met146.

Furthermore, by soaking CphA crystals in a biapenem solution, a reaction intermediate could be trapped into the active site of the enzyme [16]. The analysis of this structure allowed us to select several residues potentially important for substrate binding such as Val67, Thr157, Lys224 and Lys226, respectively (figure 1).

The side-chain of Val67 is in van der Waals contact with the 1β-methyl group of biapenem. Val67 is a residue of the L1 loop (Tyr60-Val67) [13, 16] and is part of the "hydrophobic wall" which defines the active site of CphA. The Val67 residue is conserved in B2 metallo-β-lactamases and in the BcII, CcrA and IMP-1 B1 enzymes [13]. The hydroxyl group of Thr157 makes hydrogen bonds with the hydroxyethyl group on C6 of biapenem and, after hydrolysis, with the newly formed carboxylate group [16]. Thr157, a residue of the α3 helix located near the active site groove, is only conserved in subclass B2 enzymes. As in CcrA and IMP-1 subclass B1 enzymes [21, 30-33], the Lys224 side-chain forms an electrostatic interaction with the invariant carboxylate group on C3 of the β-lactam. It is conserved in B2 and B1 enzymes with the exception of VIM-2 [13]. The Lys226 side chain is the only charged side chain near the C2 bicyclotriazoliumthio group of biapenem.

In order to evaluate their importance in metal binding and/or catalysis, substitutions of residues potentially involved in zinc binding have been performed by site-directed mutagenesis (H118A, D120A, D120T, H196A and H263A). To examine the effects of the charge or size of the residues on the substrate specificity, valine at position 67 was replaced by Ala, Ile and Asp, threonine at position 157 by Ala, lysine residues at positions 224 and 226 by Gln. Lys224 was also replaced by Gln in the N116H-N220G extended spectrum double mutant [34].

Experimental

Bacterial strains and vectors

Escherichia coli DH5α (Stratagene Inc., La Jolla, Calif.) and *E. coli* BL21 (DE3) pLysS Star (Invitrogen, Merelbeke, Belgium) were used as hosts for the construction of the different expression vectors and for the production of β-lactamases, respectively. pET9a-CphA [35] was used as plasmid template in the PCR site-directed mutagenesis amplifications. pK18-CphA vector was constructed by a ligation of the *Eco*RI-*Sma*I fragment of pAS20R [4] and the *Sma*I-*Hind*III fragment of pET9a-CphA [35] in position *Eco*RI-*Hind*III of the polylinker of the pK18 vector [36]. Moreover, a unique *Pst*I restriction site was introduced by site-directed mutagenesis at the end of the signal peptide coding sequence. The CphAPstIa and CphAPstIb primers used for this purpose are described in the supplementary material section. pK18-CphA was then used as template in the pentapeptide scanning reaction [37] described below.

Chemicals and antibiotics

The primers used for the mutagenesis were synthesized by Eurogentec (Liège, Belgium). Kanamycin was purchased from Merck (Darmstadt, Germany). Imipenem ($\Delta\varepsilon_{300}$ = -9000 M^{-1} cm^{-1}) was from Merck Sharp and Dohme Research Laboratories (Rahway, NJ, USA), biapenem ($\Delta\varepsilon_{294}$ = -9900 M^{-1} cm^{-1}) from Shionogi Pharmaceutical Co., (Osaka, Japan), ampicillin, benzylpenicillin ($\Delta\varepsilon_{235}$ = -775 M^{-1} cm^{-1}), cephaloridine ($\Delta\varepsilon_{260}$ = -10000 M^{-1} cm^{-1}), cefotaxime ($\Delta\varepsilon_{260}$ = -7500 M^{-1} cm^{-1}) from Sigma (St Louis, Mo., USA) and nitrocefin ($\Delta\varepsilon_{482}$ = -15000 M^{-1} cm^{-1}) from Unipath Oxoid (Basingstoke, UK). The variations of the molar extinction coefficient upon β-lactam hydrolysis are from references [38] (biapenem) and [39]. The antibiotics used in this study are illustrated in figure 1 (biapenem) and in the supplementary material section.

Site-directed mutagenesis

The Quick Change Site-directed mutagenesis kit (Stratagene Inc., La Jolla, Calif.) was used to introduce all the mutations. The primers designed for these experiments are listed as supplementary material. The mutants were constructed using pET9a-CphA WT as template. The triple mutant N116H-N220G-K224Q was constructed using pET9a-N116H-N220G mutant [34] as template. The introduction of the desired mutations and the absence of additional unwanted mutations were always verified by sequence analysis.

Pentapeptide scanning

A pentapeptide scanning reaction [37] was performed with the help of the GPS^{TM} –LS Scanning System (New England Biolabs, Hitchin, UK). This system allows the insertion of 15 bp linkers at random positions throughout the *blaCphA* gene of the pK8-CphA plasmid. The different plasmids were used to transform *E. coli* DH5α by electroporation. The colonies were selected on LB-agar plates supplemented by 50 µg/ml kanamycin and 10 µg/ml imipenem, and 50 µg/ml kanamycin and 8 µg/ml benzylpenicillin, respectively. The plasmids were prepared and the different *blaCphA* genes sequenced to determine the positions of the insertion.

Protein expression and purification

The genes encoding the mutant proteins were cloned into pET9a using *BamH*I and *Nde*I restriction sites. The different vectors were then introduced into *E. coli* strain BL21 (DE3) pLysS Star. Overexpression and purification of mutant proteins were performed as described for the wild-type protein [15, 27, 35] with the following modification. Bacteria expressing the wild-type protein were grown for 8 h at 37 °C in 2XYT medium while those expressing the mutants were grown for 24 h at 18 °C in the same medium. This temperature was made necessary by the fact that the mutants were produced mainly in a non-soluble form (inclusion bodies) when the cultures were grown at 37 °C.

ESI-MS and Metal Content Determination

Samples of wild-type and mutant CphA enzymes were equilibrated in 10 mM ammonium acetate buffer (pH 6.5) by centrifugal filtration prior to ESI-MS. For each protein mass spectra were obtained under both denaturing and native conditions. Denaturation of the protein was performed by dilution of the protein to a final concentration of 2-5 µM in a 50:50 (v/v) water/acetonitrile mixture containing 0.1% formic acid. The native protein was diluted to 10 - 15 µM in 10 mM ammonium acetate.

All mass spectra were acquired on a Q-TOF1 mass spectrometer (Micromass, UK) equipped with a nano-ESI source using Au/Pd coated borosilicate needles purchased from Protana (Odense, Denmark). Capillary voltage was set at 1250 V and cone voltage at 40 V and 60 V for the denatured and native proteins respectively. Acquisition time was 3 to 5 min across an m/z range of 400 - 3000. The mass spectra were processed with MassLynx v3.1 software of Micromass. The instrument was calibrated using a mixture of myoglobin and trypsinogen. The zinc content of each protein was derived from the mass difference between the native and denatured proteins.

Determination of the zinc content using ICP/MS

Protein samples were dialyzed against 15 mM sodium cacodylate pH 6.5. Protein concentrations were determined by measuring the absorbance at 280 nm (ε_{280} = 38500 M^{-1} cm^{-1}). Zinc contents were determined by Inductively Coupled Plasma Mass Spectroscopy (ICPMS) as previously described [15, 27].

Stability toward chaotropic agents

The stability of the different proteins was studied by fluorescence. The wild-type and mutant enzymes (0.05 mg/ml) were incubated for 16h in the presence of increasing urea concentrations (0-8M) at 4°C. Fluorescence emission spectra of the

enzymes were recorded at 20°C with a Perkin Elmer LS50B luminescence spectrometer using excitation and emission wavelengths of 280 and 333 nm, respectively.

Circular dichroism

Circular dichroism spectra of the different enzymes (0.5 mg/ml) were obtained using a JASCO J-810 spectropolarimeter. The spectra were scanned at 20°C with 1 nm steps from 200 to 250 nm (far UV) and from 250 to 310 nm (near UV).

Determination of kinetic parameters

The hydrolysis of the antibiotics was monitored by following the absorbance variation resulting from the opening of the β-lactam ring, using an Uvikon 860 spectrophotometer equipped with thermostatically controlled cells and connected to a microcomputer. For biapenem, imipenem, benzylpenicillin, nitrocefin, cephaloridine and cefotaxime, the wavelengths were 294, 300, 235, 482, 260 and 260 nm, respectively. Cells with 0.2 – 1.0 cm pathlengths were used, depending on the substrate concentrations. When the K_m values of the studied enzymes were sufficiently high, the k_{cat} and K_m parameters were determined either under initial-rate conditions, using the Hanes linearization of the Henri-Michaelis-Menten equation, or by analysing the complete hydrolysis time courses [40]. Low and very high K_m values were determined as K_i's using imipenem or nitrocefin as reporter substrates. In the cases of low K_m values, the k_{cat} values were obtained from the initial hydrolysis rates measured at saturating substrate concentration, and in the cases of high K_m values, k_{cat} was derived from the k_{cat}/K_m ratio. All experiments were performed at 30° C in 15mM sodium cacodylate buffer pH 6.5.

Inactivation by EDTA

Inactivation of CphA and the H118A, H196A, H263A and D120A mutants by EDTA was studied in 15 mM sodium cacodylate, pH 6.5 at 30°C, using 200 µM imipenem as the reporter substrate and in the presence of different concentrations of

EDTA in a total volume of 0.5 ml. Since the inactivation time courses followed pseudo-first-order kinetics, the rate constants characterizing the inactivation of the enzyme were calculated from the dependence of the pseudo-first-order constant k_i upon the chelating agent concentration on the basis of the following model:

$$E.Zn + C \underset{}{\overset{K}{\rightleftharpoons}} E.Zn.C \underset{k_{-2}}{\overset{k_{+2}}{\rightleftharpoons}} E + Zn.C$$

in which E.Zn, C, E.Zn.C, E, and Zn.C are the metalloenzyme, the chelator, a ternary metalloenzyme-chelator complex, the apoenzyme, and the metal-chelator complex, respectively. K is the dissociation constant of the E.Zn.C ternary complex, k_{+2} the individual rate constant for the dissociation of E.Zn.C into E + Zn.C and and k_{-2} the association constant, which was negligible in the case of the H263A mutant.

As [Zn.C] is higher than [E], the ternary complex formation from the apoenzyme and the zinc-chelatant complex is characterized by a pseudo-first-order constant:

$k_{-2}' = k_{-2}[Zn.C]$

The individual values of K and k_{+2} were determined by fitting the values of k_i to equation 1

$$k_i = \frac{k_{+2}[C]}{K[(K_m + [S])/K_m] + [C]} + k_{-2'} \quad \text{(Eq. 1)}$$

where [S] and K_m were the concentration and the K_m value of the reporter substrate, respectively.

Enzymatic measurement in the presence of increasing concentrations of zinc and determination of K_{D2}

Residual activity in the presence of increasing concentrations of zinc was measured at 30°C in 15mM sodium cacodylate pH 6.5 as already described [27].When binding of the second zinc ion resulted in a complete loss of activity, the data were analysed according to Eq.2 [27]:

$RA = [K_{D2} / ([Zn] + K_{D2})] \times 100$ (Eq. 2)

where RA is the residual activity and K_{D2} is the dissociation constant for the second zinc ion.

When binding of the second zinc ion resulted in an incomplete loss of activity or in an increase of activity, Eq.3 was used [27]:

$RA = [(K_{D2}+\alpha[Zn])/([Zn]+K_{D2})] \times 100$ (Eq. 3)

where α represents the ratio of activity at saturating zinc concentration versus activity in the absence of added zinc (Act. $[Zn]_{(\infty)}$ / Act. $[Zn]_{(0)}$).

Experimental data were fitted to Eq.2 or 3 by non-linear regression analysis with the help of the Sigma Plot software.

Results and discussion

A mutant that presents a Leu-Phe-Lys-His-Val insertion located just after Val67 ($V67_{LFKHV}$) was obtained by a pentapeptide scanning experiment. The *E. coli* DH5α cells transformed by pK18-CphA $V67_{LFKHV}$ were unable to grow on LB-agar plates supplemented by 10 µg/ml imipenem, in contrast to bacteria producing the wild-type enzyme. These cells were also unable to grow in the presence of 8 µg/ml ampicillin. The $V67_{LFKHV}$ mutant was produced in the periplasmic fraction of *E. coli* DH5α (result not shown).

The different mutants were expressed in *E. coli* BL21 (DE3) pLysS Star and purified to homogeneity. The presence of the mutations was verified by mass spectrometry (table 1). Within experimental errors, the mutants were found to exhibit the expected masses, with the exception of $V67_{LFKHV}$ mutant which presented a mass deficit of 92 Da. The N-terminal sequence of this mutant showed that there is no amino acid loss at the N-terminal side. The difference between the calculated and measured masses could thus be due to the loss of the C-terminal serine.

The stability of the different mutants against urea as denaturating agent was similar to that of the wild-type enzyme ($C_{1/2}$ = 2.7 – 3 M) except for T157A ($C_{1/2}$ = 2.2 M) and H263A ($C_{1/2}$ = 2.4 M) mutants which turned out to be a little less stable.

All the mutants had far-UV CD spectra superimposable on that of wild-type CphA (not shown). The tertiary structures were conserved for H118A and H196A while the environment of one or more aromatic residues was modified in H263A, D120A and D120T when compared to the wild-type enzyme (supplementary material). Near-UV CD spectra and fluorescence emission spectra of the N116H-N220G-K224Q and $V67_{LFKHV}$ mutants suggested a small conformation change in the protein tertiary structure (not shown). Such a small conformation change had already been observed for the N116H-N220G double mutant [34].

The activities of the mutants were measured against several compounds representing the three major families of β-lactam antibiotics, namely carbapenems, penicillins and cephalosporins, in the absence of added zinc (free zinc concentrations below 0.4 µM) (tables 3 and 5). Under these conditions, all the mutants, except $V67_{LFKHV}$, were shown to contain one zinc ion, as does the wild-type enzyme (tables 1

and 2). $V67_{LFKHV}$ already exhibited a di-zinc form (30 %) in conditions where the wild-type enzyme is only mono-zinc (table 1).

I. Mutational analysis of zinc binding sites

Although His118 and His196 are not involved in the binding of the catalytic metal ion [16], their replacement by Ala drastically reduces the enzymatic activity, suggesting important roles for these residues in the catalytic mechanism. The H118A and H196A mutations lead to an at least 1000-fold decrease in the activity against carbapenems compared to the wild-type enzyme (table 3). This result is perfectly in agreement with the structural data. Garau *et al*. suggested that His118 is the general base which activates the hydrolytic water molecule and that His196 contributes to the oxyanion hole by forming a hydrogen bond with the carbonyl oxygen of the β-lactam bond. Moreover, these residues might stabilize the carboxylate which is formed upon hydrolysis of the substrate [16]. This "active role" of His118 and His196 contrasts with the results obtained for Asn116, which in subclass B2 enzymes replaces His116, one of the zinc ligands in B1 and B3 enzymes. Indeed, whereas the His116Ser replacement reduces the activity of the B1 *Bacillus cereus* enzyme 15-20 fold, the Asn116Ser replacement in CphA yielded an enzyme whose catalytic and zinc-binding properties were similar to those of the wild-type enzyme. These results indicate that Asn116 in B2 enzymes is not a "functional substitute" of His116 in B1 and B3 [27].

After replacement of Asp120 and His263 by residues which cannot serve as zinc ligands, the mutant proteins could still bind one zinc ion but are also catalytically impaired in a dramatic manner. The D120A, D120T and H263A mutations result in a very large decrease in the activities against carbapenems (at least 50 000 fold) mainly due to strongly decreased k_{cat} values (table 3). This very low residual activity could be explained by a poor positioning of the Zn^{2+} ion in the active site of the mutants and a deformation of its coordination sphere. In this respect, it is interesting to note that the Asn220Gly mutation, which does not directly affect any of the zinc ligands but is situated next to Cys221, causes a displacement of the latter in 20 % of the molecules [16].

ICP/MS shows that, in contrast to the wild-type enzyme, these five mutant enzymes remain in their mono-zinc forms even in the presence of 100 µM free zinc (table 2).

The effect of the zinc ion concentration on the activity has also been studied. The binding of the second zinc ion is severely affected by the His118Ala and His196Ala mutations (figure 2a). From these curves, the H118A and H196A mutants are found to exhibit much higher K_{D2} values (940 ± 80 and 1250 ± 50 µM respectively) than the wild-type enzyme (46 ± 3 µM). The poorer binding of the second zinc by CphA H118A was also demonstrated by mass spectrometry, which failed to detect the di-zinc form of this mutant [41]. This indicates that both histidine residues are involved in the binding of the second, inhibitory, zinc ion.

This interpretation is in disagreement with the conclusions of Crawford *et al.* [28] that the inhibitory zinc binds at a distance of at least 0.5 nm from the catalytic one in the ImiS B2 enzyme. Our results could be reconciled with this hypothesis if both our mutations resulted in significant conformational changes. On the basis of CD data (supplementary material), this does not seem to be the case. Costello *et al*. have shown that the inhibitory zinc is bound by a sulphur [29]. The sulphur ligand in the inhibitory site should come from a methionine residue, since the only cysteine residue (Cys221) is a ligand of the first zinc ion. The mutation of Met146 to isoleucine abolishes metal inhibition. However, mutations of other CphA residues, which have not been implicated as ligands of the second zinc ion, can have similar effects (lower inhibition or even activation by excess of zinc, as observed in the part "Mutational analysis of putative substrate binding site residues" of the present work). Moreover, a careful examination of the CphA 3D structure indicates that His118 and Met146 are poorly positioned to bind the same zinc ion. The distance between their Cα's is 7.57 Å, while the distances between the sulphur of Met146 and the nitrogens of the imidazole group of His118 are 10.40 and 10.91Å respectively. Also, the space between these residues does not allow the accommodation of a zinc ion because it is occupied by the backbone of the Asn114-His118 loop connecting strand β6 and helix α2.

Moreover, an involvement of His118 and His196 in the binding of the inhibitory zinc ion makes sense in the light of the strongly decreased activity of the mutants (table 3)

since this binding would prevent them from playing their catalytic roles in the hydrolysis of carbapenems.

According to the structure, the presence of a second zinc ion in the active site interacting with His118 and His196 would not require any major rearrangement. There is indeed a free space between those residues and Cys221, Asp120 and Asn116. This second zinc ion would approximately be located at a position similar to that of the first zinc ion in the subclasses B1 and B3 β-lactamases and two of the zinc ligands would be conserved. Compared to the available structure of CphA, the only modification needed would be a 180° rotation around the Cβ-Cγ bond of the His196 side chain to bring the Nε2 atom in the right orientation (figures 3a and 3b).

From this crude modelling, the identity of the third ligand of the second zinc ion is not clear. However, the fact that the Cys221 CphA mutants no longer bind zinc [27] while mutants of the two other ligands (Asp120 and His263) of the first zinc binding site retain relatively high affinities for zinc (K_D < 0.4 μM) points towards a role of Cys221 in the binding of both zinc ions. The role of a cysteine in the simultaneous binding of two zinc ions is a known feature that has for example been observed in the structure of the DNA-binding domain of the Gal4 transcription factor [42]. The second zinc binding site described here would likely be more energetically favourable (one side chain rotation) than the major rearrangement required to organise a zinc binding site involving the embedded Met146. The presence of a sulphur in the second binding site that lead to the identification Met146 could maybe be explained by the involvement of Cys221 in the binding of both ions.

The affinities of the Asp120 and His263 mutants are nonetheless probably decreased when compared to that of the wild-type enzyme as indicated by the higher rates of inactivation by EDTA (table 4). They are probably between those observed for site 1 and site 2 in the wild-type enzyme for which the K_{D1} is below 10 pM [43] and K_{D2} is 46 μM [15]. Because the residual activity of these mutants can be inhibited by EDTA and because the K_{D2}'s deduced from the inhibition by zinc are still relatively close to 46 μM (figure 2b) (K_{D2} values are 15 ± 1.5 μM for H263A and 44 ± 6 and 41 ± 2 μM for D120A and D120T respectively), the binding of the first zinc to these mutants might result from a reduced affinity for site 1 rather than an improved affinity for the inhibitory site 2. The occupation of both sites at the same time has not been observed [41].

II. Mutational analysis of putative substrate binding site residues

Our kinetic results are in good agreement with the crystallographic structure of CphA in complex with biapenem [16] and confirm the importance of the Val67 residue for the binding of this substrate into the active site of CphA. The K_m values of V67I and V67D for biapenem strongly increase, so that only k_{cat}/K_m could be measured (table 5). This phenomenon could be due to a less favourable interaction with the 1-β-methyl group of the antibiotic. In addition, we show that a hydrophobic interaction between Val67 and the C2 methyl groups of penicillin is likely, since the K_m value of V67D for benzylpenicillin is larger than that of the wild-type CphA enzyme (table 5). A similar interaction has already been proposed between the BcII subclass B1 enzyme and benzylpenicillin [44]. Moreover, Simona *et al*. have recently suggested a possible role of the L1 loop (Tyr60-Val67) for the mechanism of binding carbapenem molecules [45].

As for the wild-type CphA [15], the binding of a second zinc ion inhibits in a non-competitive manner the hydrolysis of imipenem by the Val67 mutants. The dissociation constants for the second zinc ion are similar to that of wild-type enzyme for V67I and V67D (46 ± 3 µM) or slightly reduced for V67A (16 ± 3 µM).

The $V67_{LFKHV}$ mutant, with a five-residue insertion just after Val67, presents a strongly decreased affinity for biapenem, imipenem and nitrocefin (table 5). The extended loop might fold above the active site groove and in this way reduce the active site accessibility. The lengthening of the L1 loop and/or the introduction of a charged residue (Lys) could have a negative effect on the affinity of the enzyme for its substrate. The apparent dissociation constant for the second zinc ion is below 1 µM whereas it is 46 µM for the wild-type CphA. Together with the fact that this mutant exhibits a di-zinc form (30 %) in conditions where the wild-type enzyme is only mono-zinc, this result suggests that the His residue in the inserted pentapeptide might probably interact with the second zinc ion, thus recreating a possible second "3 His" zinc binding site ($His67_d$-His118-His196). However, a significant rearrangement would be necessary in order to bring the additional histidine into sufficiently close proximity to His118 and His196. Consequently, this hypothesis should be confirmed by EXAFS and PAC experiments and by the resolution of the 3D structure.

Various modifications can broaden the activity spectrum of the strict CphA carbapenemase. The N116H-N220G extended-spectrum mutant was obtained by a site-directed approach on the basis of sequence alignments between members of the B2 and B1 subclasses [34]. In the present study, surprisingly, the replacement of Thr157 by an alanine results in a significant modification of the activity spectrum of the enzyme, since the catalytic efficiency of this mutant *versus* benzylpenicillin, cefotaxime and nitrocefin is larger than that of the wild-type enzyme. However, although T157A is far from being as efficient as the N116H-N220G mutant [34], it retains, in contrast, a good activity versus imipenem (table 5).

Thr157 does not seem to play an important role in the CphA catalytic mechanism, but according to the structure of CphA in complex with modified biapenem (PDB code 1X8I) and the proposed mechanism for enzymatic activity on carbapenems [16], the C6 (C7 for cephalosporins) side chains of β-lactam antibiotics are likely located in the environment of Thr157 during hydrolysis. A residue with a slightly reduced bulkiness could therefore be more suited to accommodate the larger and differently oriented side chain of most β-lactam antibiotics compared to carbapenems. This could explain the more extended spectrum observed for this mutant. Because the T157A mutant only retains a good activity against imipenem while the interactions of imipenem and biapenem with Thr157 should be affected similarly, we believe that this residue is more important for the optimum positioning of the substrate than for its affinity for the active site. The bulkier and more rigid biapenem would therefore need an extra anchoring to be perfectly oriented while imipenem would fit more naturally into the active site.

Zinc ions inhibit the hydrolysis of imipenem and benzylpenicillin by T157A in a non-competitive manner, but the di-zinc form of this mutant retains 40 % of activity *versus* benzylpenicillin while it is practically completely deprived of activity *versus* imipenem (figure 4a). The dissociation constants for the second zinc ion are similar for both substrates and similar to that of the wild-type enzyme (respectively 46 ± 3 µM for T157A and imipenem, 55 ± 11 µM for T157A and benzylpenicillin and 46 ± 3 µM for the wild-type enzyme and imipenem [15]). In contrast to the N116H-N220G mutant [34], imipenem and benzylpenicillin seem in this case to be hydrolyzed via the same mechanism. The activity of the wild-type CphA against benzylpenicillin is too

low to allow meaningful measurements, however zinc also behaves as an inhibitor in this case.

Our kinetic results show that Lys224 is important for the binding of β-lactam antibiotics into the active site of CphA, as already observed for the subclass B1 enzymes CcrA and IMP-1 [21, 30-33]. The K224Q mutant exhibits a decreased catalytic efficiency *versus* carbapenem substrates when compared to the wild-type enzyme. The individual k_{cat} and K_m values could not be determined. In the same way, the K_m value for benzylpenicillin strongly increases (table 5). This role is in good agreement with the crystallographic structure of CphA in complex with biapenem which shows an electrostatic interaction between Lys224 and the invariant C3 carboxylate of the β-lactam antibiotic and with the simulations of Xu and his co-workers [46].

The N116H-N220G-K224Q triple mutant presents increased K_m values and decreased k_{cat} values when compared to the N116H-N220G double mutant (table 5). This triple mutant, while significantly less active than the N116H-N220G double mutant, retains a relatively extended spectrum when compared to the wild-type enzyme. It is particularly interesting since, as already observed for the N116H-R121H-N220G triple mutant [34] and in contrast to the wild-type enzyme, added zinc behaves as an activator. The hydrolysis rate of imipenem and nitrocefin by the N116H-N220G-K224Q triple mutant strikingly increases 1.6 and 2.5-fold at saturating Zn^{2+} concentration (figure 4b). The dissociation constant for the second zinc ion determined for this triple mutant (4.0 ± 1.1 µM and 1.6 ± 0.2 µM with imipenem and nitrocefin respectively as substrates) is similar to that of the N116H-N220G double mutant (5.0 ± 0.9 µM [34]). For all the other mutants, the hydrolysis of nitrocefin is independent of zinc concentration.

This phenomenon remains difficult to explain in the absence of structural data on the di-zinc inhibited form of the wild-type enzyme but it is quite likely that binding of the second zinc ion induces distinct structural changes in the wild-type and mutant proteins.

The replacement of Lys226 only affects the kinetic parameters of biapenem. Although the k_{cat} value is increased, the catalytic efficiency remains similar to that of the wild-type enzyme. The K226Q mutation does not significantly modify the affinity for the second zinc ion (K_{D2} = 85 ± 10 µM).

Conclusion

Our results indicate that His118 and His196 participate in the catalytic mechanism of the subclass B2 CphA metallo-β-lactamase for which an intact Asp120-Cys221-His263 site is essential. The position of the second inhibitory zinc ion is not identified with certainty, but it is likely equivalent to the "histidine" site observed in subclasses B1 and B3 enzymes. His118 and His 196 are involved in the binding of this second zinc and Cys221 is the leading candidate as the third ligand but the geometry is maybe not optimum and Asn116 or Asp120 could play a role too.

The present study underlines the importance of Val67, Thr157 and Lys224 residues for the carbapenem binding into the active site of CphA.

Acknowledgements

This work was supported by the Belgian Federal Government (PAI P5/33), grants from the FNRS (Brussels, Belgium, FRFC grants n° 2 4508.01, 2.4.524.03 and Lot. Nat. 9.4538.03) and an European Research Training Network (MEBEL contract HPTR-CT-2002-00264). The purchase of a Jasco J-810 spectropolarimeter was supported in part by a grant from the FRFC (contract number 2.4545.01).

C.B. and F.K. were FNRS post-doctoral researchers. C.A. was the recipient of a Marie Curie fellowship.

References

1. Ambler, R.P. (1980) The structure of beta-lactamases. *Philos. Trans. R. Soc. London Ser. B*, **289**, 321-331

2. Rasmussen, B.A., Y. Gluzman, and Tally F.P. (1990) Cloning and sequencing of the class B beta-lactamase gene (ccrA) from *Bacteroides fragilis* TAL3636. *Antimicrob. Agents Chemother*. **34**, 1590-1592

3. Watanabe M., S. Iyobe, M. Inoue and Mitsuhashi S. (1991) Transferable imipenem resistance in *Pseudomonas aeruginosa*. *Antimicrob. Agents Chemother*. **35**, 147-51

4. Massidda, O., G.M. Rossolini, and Satta G. (1991) The *Aeromonas hydrophila* cphA gene: molecular heterogeneity among class B metallo-beta-lactamases. *J Bacteriol*. **173**, 4611-4617

5. Osano E., Y. Arakawa, R. Wacharotayankun, M. Ohta, T. Horii, H. Ito, F. Yoshimura and Kato N. (1994) Molecular characterization of an enterobacterial metallo beta-lactamase found in a clinical isolate of *Serratia marcescens* that shows imipenem resistance. *Antimicrob. Agents Chemother.* **38**, 71-78

6. Rossolini, G.M., N. Franceschini, M.L. Riccio, P.S. Mercuri, M. Perilli, M. Galleni, J.M. Frère, and Amicosante G. (1998) Characterization and sequence of the *Chryseobacterium (Flavobacterium) meningosepticum* carbapenemase: a new molecular class B beta-lactamase showing a broad substrate profile. *Biochem J*. **332,** 145-152

7. Chen Y., J. Succi, F.C Tenover and Koehler T.M (2003) Beta-lactamase genes of the penicillin-susceptible *Bacillus anthracis* Sterne strain. *J. Bacteriol.* **185**, 823-830

8. Felici, A., Amicosante, G., Oratore, A., Strom, R., Ledent, P., Joris, B., Fanuel, L. and Frère, J.M. (1993) An overview of the kinetic parameters of class B beta-lactamases. *Biochem.J*., **291**, 151-155

9. Prosperi-Meys, C., G. Llabres, D. de Seny, R.P. Soto, M.H. Valladares, N. Laraki, J.M. Frère, and Galleni M. (1999) Interaction between class B beta-lactamases and suicide substrates of active-site serine beta-lactamases. *FEBS Lett.* **443**, 109-111

10. Livermore, D.M. and Woodford N. (2000) Carbapenemases: a problem in waiting? *Curr. Opin. Microbiol.* **3**, 489-495

11. Walsh, T.R., M.A. Toleman, L. Poirel and Nordmann P. (2005) Metallo-β-lactamases: the quiet before the storm. *Clin. Microbiol. Rev.*, **18**, 306-325

12. Galleni, M., Lamotte-Brasseur, J., Rossolini, G.M., Spencer, J., Dideberg, O., Frère, J.M. and the Metallo-β-lactamases Working Group (2001) Standard numbering scheme for class B beta-lactamases. *Antimicrob.Agents Chemother.*, **45**, 660-663

13. Garau, G., Garcia-Saez, I., Bebrone, C., Anne, C., Mercuri, P.S., Galleni, M., Frère, J.M. and Dideberg, O. (2004) Update of the standard numbering scheme for class B beta-lactamases. *Antimicrob.Agents Chemother.*, **48**, 2347-2349

14. Segatore, B., Massida, O., Satta, G., Setacci, D. and Amicosante, G. (1993) High specificity of cphA-encoded metallo-beta-lactamase from *Aeromonas hydrophila* AE036 for carbapenems and its contribution to beta-lactam resistance. *Antimicrobial Agents and Chemother.*, **37**, 1324-1328

15. Hernandez-Valladares, M., Felici, A., Weber, G., Adolph, H.W., Zeppezauer, M., Rossolini, G.M., Amicosante, G., Frère, J.M. and Galleni, M. (1997) Zn(II) dependence of the *Aeromonas hydrophila* AE036 metallo-beta-lactamase activity and stability. *Biochemistry*, **36**, 11534-11541

16. Garau, G., Bebrone, C., Anne, C., Galleni, M., Frère, J.M. and Dideberg, O. (2005) A Metallo-beta-lactamase Enzyme in Action: Crystal Structures of the Monozinc Carbapenemase CphA and its Complex with Biapenem. *J. Mol. Biol.*, **345**, 785-795

17. Carfi, A., S. Pares, E. Duee, M. Galleni, C. Duez, J.M. Frère, and Dideberg. O. (1995) The 3-D structure of a zinc metallo-beta-lactamase from *Bacillus cereus* reveals a new type of protein fold. *Embo J.* **14**, 4914-4921

18. Concha, N.O., Rasmussen, B.A., Bush, K. and Herzberg, O. (1996) Crystal structure of the wide-spectrum binuclear zinc beta-lactamase from *Bacteroides fragilis*. *Structure*, **4**, 823-836

19. Carfi, A., Duée, E., Galleni, M., Frère, J.M. and Dideberg, O. (1998) 1.85 Å resolution structure of the zinc (II) beta-lactamase from *Bacillus cereus*. *Acta Cryst*., **D54**, 313-323

20. Fabiane, S.M., Sohi, M.K., Wan, T., Payne, D.J., Bateson, J.H., Mitchell, T. and Sutton, B.J. (1998) Crystal structure of the zinc-dependent beta-lactamase from *Bacillus cereus* at 1.9 Å resolution: binuclear active site with features of a mononuclear enzyme. *Biochemistry*, **37**, 12404-12411

21. Concha, N.O., Janson, C.A., Rowling, P., Pearson, S., Cheever, C.A., Clarke, B.P., Lewis, C., Galleni, M., Frère, J.M., Payne, D.J., Bateson, J.H. and Abdel-Meguid, S.S. (2000) Crystal structure of the IMP-1 metallo beta-lactamase from *Pseudomonas aeruginosa* and its complex with a mercaptocarboxylate inhibitor: binding determinants of a potent, broad-spectrum inhibitor. *Biochemistry*, **39**, 4288-4298

22. Garcia-Saez, I., Hopkins, J., Papamicael, C., Franceschini, N., Amicosante, G., Rossoloni, G.M., Galleni, M., Frère, J.M. and Dideberg, O. (2003) The 1.5 Å structure of *Chryseobacterium meningosepticum* zinc beta-lactamase in complex with the inhibitor, D-captopril. *J.Biol.Chem*., **278**, 23868-23873

23. Ullah, J.H., Walsh, T.R., Taylor, I.A., Emery, D.C., Verma, C.S., Gamblin, S.J. and Spencer, J. (1998) The crystal structure of the L1 metallo-beta-lactamase from *Stenotrophomonas maltophilia* at 1.7 Å resolution. *J.Mol.Biol*., **284**, 125-136

24. Garcia-Saez, I., Mercuri, P.S., Papamicael, C., Kahn, R., Frère, J.M., Galleni, M., Rossoloni, G.M. and Dideberg, O. (2003b) Three-dimensional structure of FEZ-1, a monomeric subclass B3 metallo-beta-lactamase from *Fluoribacter gormanii*, in native form and in complex with D-captopril. *J.Mol.Biol*., **325**, 651-660

25. Hernandez-Valladares, M., Kiefer, M., Heinz, U., Paul Soto, R., Meyer-Klaucke, W., Friederich Nolting H., Zeppezauer, M., Galleni, M., Frère, J.M., Rossolini, G.M., Amicosante, G. and Adolph, H.W. (2000) Kinetic and spectroscopic characterization of native and metal-substituted beta-lactamase from *Aeromonas hydrophila* AE036. *FEBS Lett.*, **467**, 221-225

26. Heinz, U., Bauer, R., Wommer, S., Meyer-Klaucke, W., Papamichaels, C., Bateson, J. and Adolph, H.W. (2003) Coordination geometries of metal ions in D- or L-captopril-inhibited metallo-beta-lactamases. *J Biol.Chem*., **278**, 20659-20666

27. Vanhove, M., Zakhem, M., Devreese, B., Franceschini, N., Anne, C. Bebrone, C., Amicosante, G., Rossolini, G.M., Van Beeumen, J., Frère, J.M. and Galleni, M.. (2003) Role of Cys221 and Asn116 in the zinc-binding sites of the *Aeromonas hydrophila* metallo-beta-lactamase. *Cell Mol Life Sci*., **60**, 2501-2509

28. Crawford, P.A., Yang, K.W., Sharma, N., Bennett, B. and Crowder, M.W. (2005) Spectroscopic studies on cobalt(II)-substituted metallo-beta-lactamase ImiS from *Aeromonas veronii* bv. *sobria*. *Biochemistry*. **44**, 5168-5176

29. Costello, A.L., N.P. Sharma, K.W. Yang, M.W. Crowder and Tierney D.L. (2006) X-ray absorption spectroscopy of the zinc-binding sites in the class B2 metallo-beta-lactamase ImiS from *Aeromonas veronii* bv. *sobria*. *Biochemistry*, **45**, 13650-13658.

30. Yang, Y., D. Keeney, X. Tang, N. Canfield and Rasmussen B.A. (1999) Kinetic properties and metal content of the metallo-β-lactamase CcrA harboring selective amino acid substitutions. *J. Biol. Chem*. **274**, 15706-15711

31. Yanchak, M.P., R.A. Taylor and Crowder M.W. (2000) Mutational analysis of metallo-β-lactamase CcrA from *Bacteroides fragilis*. *Biochemistry* **39**, 11330-11339

32. Haruta, S., Yamamoto, E.T., Eriguchi, Y. and Sawai, T. (2001) Characterization of the active-site residues asparagine 167 and lysine 161 of the IMP-1 metallo-beta-lactamase. *FEMS Microbiol Lett*. **197**, 85-89

33. Materon, I.C., Z. Beharry, W. Huang, C. Perez and Palzkill T. (2004) Analysis of the context dependent sequence requirements of active site residues in the metallo-β-lactamase IMP-1. *J. Mol. Biol.* **344**, 653-663

34. Bebrone, C., Anne, C., De Vriendt, K., Devresse, B., Van Beeumen, J., Frère, J.M. and Galleni, M. (2005) Dramatic broadening of the substrate profile of the *Aeromonas hydrophila* CphA metallo-β-lactamase by site-directed mutagenesis, *J. Biol. Chem*.,**17**, 180-188

35. Hernandez-Valladares, M., Galleni, M., Frère, J.M., Felici, A., Perilli, M., Franceschini, N., Rossolini, G.M., Oratore, A. and Amicosante, G. (1996) Overproduction and purification of the *Aeromonas hydrophila* CphA metallo-beta-lactamase expressed in *Escherichia coli*. *Microbial Drug Resistance* **2(2)**, 253-256

36. Pridmore, R.D. (1987) New and versatile cloning vectors with kanamycin-resistance marker. *Gene*. **56**, 309-312

37. Hallet, B., Sherrat, D.J. and Hayes, F. (1997) Pentapeptide scanning mutagenesis: random insertion of a variable five amino acid cassette in a target protein. *Nucleic Acids Res*. **25**:1866-1867

38. Mercuri, P.S., Garcia-Saez, I., De Vriendt, K., Thamm, I., Devreese, B., Van Beeumen, J., Dideberg, O., Rossolini, G.M., Frère, J.M. and Galleni, M. (2004) Probing the specificity of the sub-class B3 FEZ-1 metallo-beta-lactamase by site-directed mutagenesis. *J. Biol. Chem*. **279**:33630-33638

39. Matagne, A., Dubus, A., Galleni, M. and Frère, J.M. (1999) The beta-lactamase cycle: a tale of selective pressure and bacterial ingenuity. *Nat Prod Rep*. **16**:1-19

40. De Meester, F., Joris, B., Reckinger, G., Bellefroid-Bourguignon, C., Frère, J.M. and Waley, S.G. (1987) Automated analysis of enzyme inactivation phenomena. Application to beta-lactamases and DD-peptidases. *Biochem.Pharmacol*., **36**, 2393-2403

41. De Vriendt, K., Van Driessche, G., Devreese, B., Bebrone, C., Anne, C., Frère, J.M., Galleni, M. and Van Beeumen, J. (2006) Monitoring the Zinc Affinity of the Metallo-beta-Lactamase CphA by Automated nanoESI-MS. *J. Am. Soc. Mass. Spectrom*. **17**, 180-188

42. Baleja, J.D., Thanabal, V. and Wagner, G. (1997) Refined solution structure of the DNA-binding domain of GAL4 and use of 3J(113Cd,1H) in structure determination. *J. Biomol. NMR* **10**, 397-401

43. Wommer, S., Rival, S., Heinz, U., Galleni, M., Frère, J.M., Franceschini, N., Amicosante, G., Rasmussen, B., Bauer, R. and Adolph H.W. (2002) Substrate-activated zinc binding of metallo-beta-lactamases: physiological importance of mononuclear enzymes. *J. Biol. Chem*. **277**, 24142-24147

44. Prosperi-Meys, C., D. de Seny, G. Llabres, M. Galleni and Lamotte-Brasseur J. (2002) Active-site mutants of class B β-lactamases: substrate binding and mechanistic study. *Cell. Mol. Life Sci*. **59**, 2136-2143

45. Simona, F., A. Magistrato, D.M.A Vera, G. Garau, A.J. Vila and Carloni P. (2007) Protonation state and substrate binding to B2 metallo-β-lactamase CphA from *Aeromonas hydrophila*. *Proteins* **69**, 595-605

46. Xu, D., D. Xie and Guo H. (2006) Catalytic mechanism of class B2 metallo-β-lactamase. *J. Biol. Chem*. **281**, 8740-8747

Tables

Table 1. Masses and metal binding for WT CphA and mutants.

Protein	Assay conditions	Calculated mass (Da)	Measured mass (Da)	Mass difference (Da)	N° of Zn^{2+} ions[a]
WT	Native		25253.5	63.9	1
	Denatured	25189	25189.6		
H118A	Native		25187.6	62.8	1
	Denatured	25123	25124.8		
D120A	Native		25206.7	61.6	1
	Denatured	25146	25145.1		
D120T	Native		25237.3	62.2	1
	Denatured	25176	25175.1		
H196A	Native		25187.6	62.9	1
	Denatured	25123	25124.7		
H263A	Native		252185.1	62.7	1
	Denatured	25123	25122.4		
V67A	Native		25223.3	62.9	1
	Denatured	25161	25160.4		
V67I	Native		25265.1	60.8	1
	Denatured	25203	25204.3		
V67D	Native		25266.9	62.1	1
	Denatured	25205	25204.8		
V67$_{LFKHV}$	Native		25874.8	62.4	1 (70 %)
			25936.3	123.9	2 (30 %)
	Denatured	25904 (25815)*	25812.4		

T157A	Native		25221.7	63.3	1
	Denatured	25159	25158.4		
K224Q	Native		25251.8	61.7	1
	Denatured	25189	25190.1		
K226Q	Native		25252.5	63.7	1
	Denatured	25189	25188.8		
N116H-R121H-K224Q	Native		25218.8	62.7	1
	Denatured	25155	25156.1		

* The value between round brackets is obtained by assuming the elimination of the C-terminal serine. [a] The average mass of Zn^{++} is 65.4. However, two or more protons can be displaced upon protein binding, giving the bound Zn^{++} an apparent mass of 63.4.

Table 1 (continued)

Table 2. Summary of zinc binding for wild-type CphA and the H118A, H196A, H263A, D120A, D120T mutants.

SD values were below 10%. N.D.: not determined.

Protein	$[Zn^{2+}] \leq 0.4$ µM		$[Zn^{2+}] = 100$ µM	
	MS	ICP-MS	MS	ICP-MS
WT	1	1.0	2	1.9
H118A	1	0.9	N.D.	1.2
H196A	1	N.D.	N.D.	1.2
H263A	1	1.0	N.D.	0.9
D120A	1	1.3	N.D.	1.3
D120T	1	1.3	N.D.	1.3

Table 3. Kinetic parameters of the wild-type CphA enzyme and the H118A, H196A, H263A, D120A and D120T mutants. Measurements were done at 30 °C in 15 mM sodium cacodylate pH 6.5. SD values were below 10%. N.D.: not determined. Values for the wild-type enzyme are from Vanhove *et al*., 2003 [27].

Enzyme	**Substrate**	**k_{cat} (s^{-1})**	**K_m (µM)**	**k_{cat}/K_m ($M^{-1}s^{-1}$)**
WT	Imipenem	1200	340	3 500 000
	Biapenem	300	170	1 800 000
	Benzylpenicillin	0.03	870	35
	Nitrocefin	0.008	1300	6
	Cephaloridine	< 0.006	6000	< 1
H118A	Imipenem	2.4	1150	2100
	Biapenem	0.1	730	150
	Benzylpenicillin	0.007	210	33
	Nitrocefin	0.005	30	170
	Cephaloridine	> 0.01	> 4500	2.2
H196A	Imipenem	16	4300	3700
	Biapenem	N.D.	N.D.	N.D.
	Benzylpenicillin	> 0.1	> 5000	20
	Nitrocefin	0.006	15	400
	Cephaloridine	> 0.11	> 4500	24
H263A	Imipenem	0.02	1700	12
	Biapenem	> 0.005	> 1500	3
	Benzylpenicillin	N.D.	N.D.	N.D.
	Nitrocefin	0.003	15	200
	Cephaloridine	N.D.	N.D.	N.D.
D120A	Imipenem	0.024	330	73
	Biapenem	0.0015	100	15
	Benzylpenicillin	N.D.	N.D.	N.D.
	Nitrocefin	0.0024	26	92
	Cephaloridine	N.D.	N.D.	N.D.
D120T	Imipenem	0.025	210	120
	Biapenem	N.D.	N.D.	N.D.
	Benzylpenicillin	N.D.	N.D.	N.D.
	Nitrocefin	0.0002	50	4
	Cephaloridine	N.D.	N.D.	N.D.

Table 4. Individual parameters for the inactivation of WT, H118A, H196A, H263A and D120A CphA by EDTA.

SD values were below 10%.

	K (mM)	k_{+2} (s^{-1})	k_{-2} (s^{-1})	k_{+2}/K ($M^{-1}s^{-1}$)
WT	5.5	0.007	0.0014	1.3
H118A	5.2	0.002	0.003	0.4
H196A	16.4	0.008	0.005	0.5
H263A	0.01	0.005	/	500
D120A	0.5	0.003	0.00001	6

Table 5. Kinetic parameters of the WT, V67A, V67I, V67D, $V67_{LFKHV}$, T157A, K224Q, K226Q, N116H-N220G and N116H-N220G-K224Q CphA enzymes.

Measurements were performed at 30°C in 15 mM sodium cacodylate pH 6.5.

S.D. values are below 10 %. Values for the wild-type enzyme are from Vanhove *et al.*, 2003 [27] and values for the N116H-N220G double mutant are from Bebrone *et al.*, 2005 [34].

Enzyme	Antibiotics	k_{cat} (s^{-1})	K_m (µM)	k_{cat}/K_m ($M^{-1}s^{-1}$)
WT	Imipenem	1200	340	3 500 000
	Biapenem	300	170	1 800 000
	Benzylpenicillin	0.03	870	35
	Nitrocefin	0.008	1300	6
	Cefotaxime	> 0.0002	> 100	2
V67A	Imipenem	1000	220	4 500 000
	Biapenem	100	100	1 000 000
	Benzylpenicillin	0.004	1000	4
	Nitrocefin	0.005	26	180
V67I	Imipenem	1770	180	9 000 000
	Biapenem	> 50	> 1500	33 000
	Benzylpenicillin	0.08	730	110
	Nitrocefin	0.004	50	80
V67D	Imipenem	1280	310	4 000 000
	Biapenem	> 100	> 1500	66 000
	Benzylpenicillin	> 0.03	> 5000	6
	Nitrocefin	0.004	36	110
$V67_{LFKHV}$	Imipenem	> 30	> 1 500	20 000
	Biapenem	> 2.4	> 1500	1 600
	Nitrocefin	> 0.006	> 2 000	3
T157A	Imipenem	1680	570	3 000 000
	Biapenem	>130	> 1500	87 000
	Benzylpenicillin	1	550	1950

	Nitrocefin	0.015	110	140
	Cefotaxime	0.023	450	50
K224Q	Imipenem	> 490	> 1500	330 000
	Biapenem	> 60	> 1500	40 000
	Benzylpenicillin	> 0.03	> 5000	6
	Nitrocefin	0.007	135	52
	Cephaloridine	0.024	1000	24
	Cefotaxime	0.001	700	1.4
K226Q	Imipenem	1000	380	2 600 000
	Biapenem	1000	840	1 200 000
	Benzylpenicillin	0.004	800	5
	Nitrocefin	0.01	850	12
	Cephaloridine	0.006	1700	3.5
	Cefotaxime	0.0006	140	4.3
N116H-N220G	Imipenem	16	185	86 000
	Biapenem	5	100	50 000
	Benzylpenicillin	3.3	150	22 000
	Nitrocefin	0.7	4	180 000
	Cephaloridine	0.9	145	6 200
	Cefotaxime	0.3	50	6 000
N116H-N220G-K224Q	Imipenem	0.9	300	3 000
	Biapenem	0.26	390	670
	Benzylpenicillin	0.13	920	140
	Nitrocefin	0.2	32	6 000
	Cephaloridine	0.03	53	570
	Cefotaxime	0.015	434	34

Legends to figures

Figure 1

a) Structure of biapenem

b) Structure of the reaction intermediate

c) View of the active site of CphA in complex with the reaction intermediate.

Figure 2

Residual activity measured in the presence of increasing concentrations of zinc.

a) WT, H118A, H196A and imipenem. The curves are the best fits using Eq.2. (WT: solid, H118A: dashed, H196A: dotted).

b) WT, D120A, D120T, H263A and imipenem. The curves are the best fits using Eq.2. (WT: solid, D120A: dashed, D120T: dotted, H263A: dash-dot).

All experiments were performed at 30°C in 15 mM sodium cacodylate pH 6.5. The substrate concentration was 100 µM.

S.D. values are below 10 %.

Figure 3

Representation of the active site of the CphA enzyme

a) Structure of the mono-zinc active site PDB code 1X8G
b) Model of a di-zinc active site with addition of a Zn ion and rotation of His196 side chain as the only modification when compared to a), the dashed lines show bonds to atoms within 3 Å of Zn2

Figure 4

Residual (or relative) activity measured in the presence of increasing concentrations of zinc

a) T157A with imipenem and benzylpenicillin. The curves are the best fits using Eq.2 (imipenem, solid line) or Eq.3 (benzylpenicillin, dashed line).

b) N116H-N220G-K224Q with imipenem and nitrocefin. The curves are the best fits using Eq.3 (Imipenem: solid line, Nitrocefin: dashed line).

All experiments were performed at 30°C in 15 mM sodium cacodylate pH 6.5.

The substrate concentrations were 100 μM for imipenem, 1 mM for benzylpenicillin and 100 μM for nitrocefin.

S.D. values are below 10 %.

Figures

Figure 1 (Bebrone *et al.*)

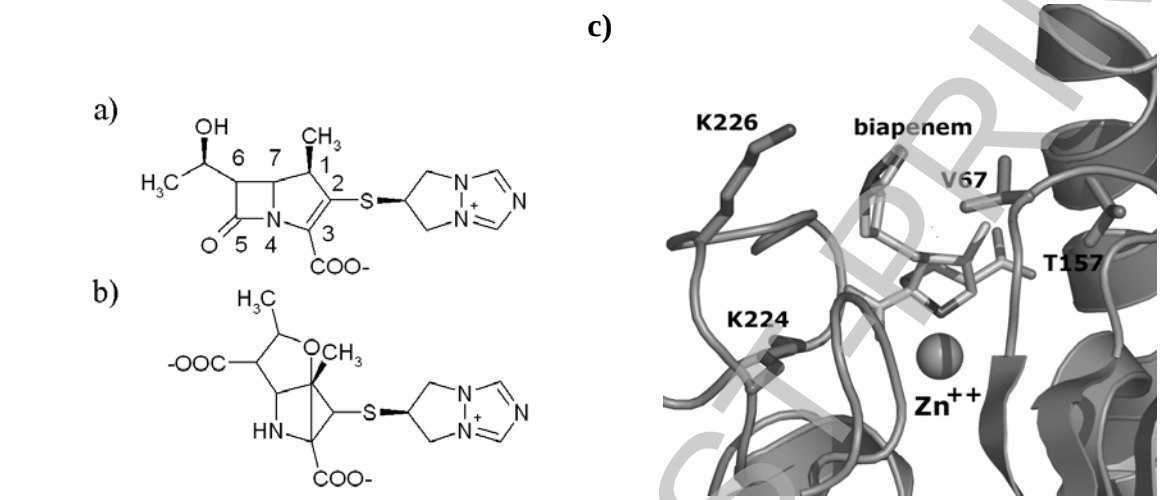

Figure 2 (Bebrone *et al.*)

a)

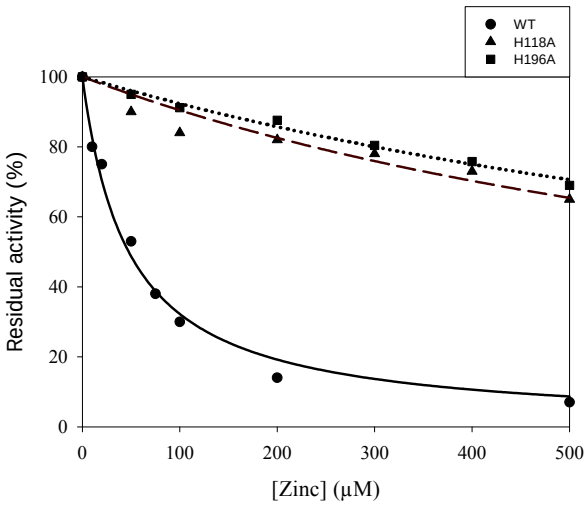

b)

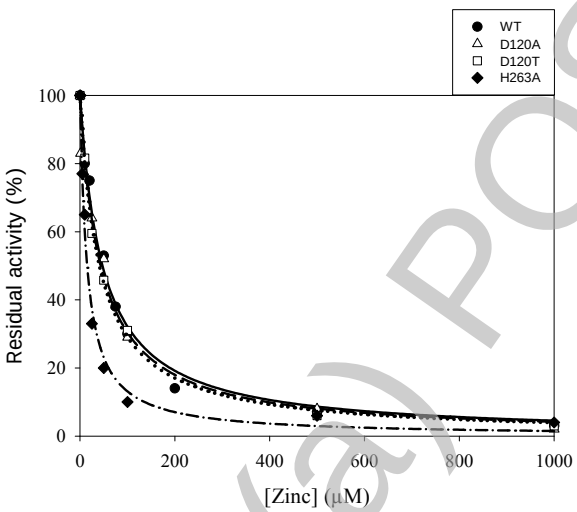

Figure 3 (Bebrone *et al.*)

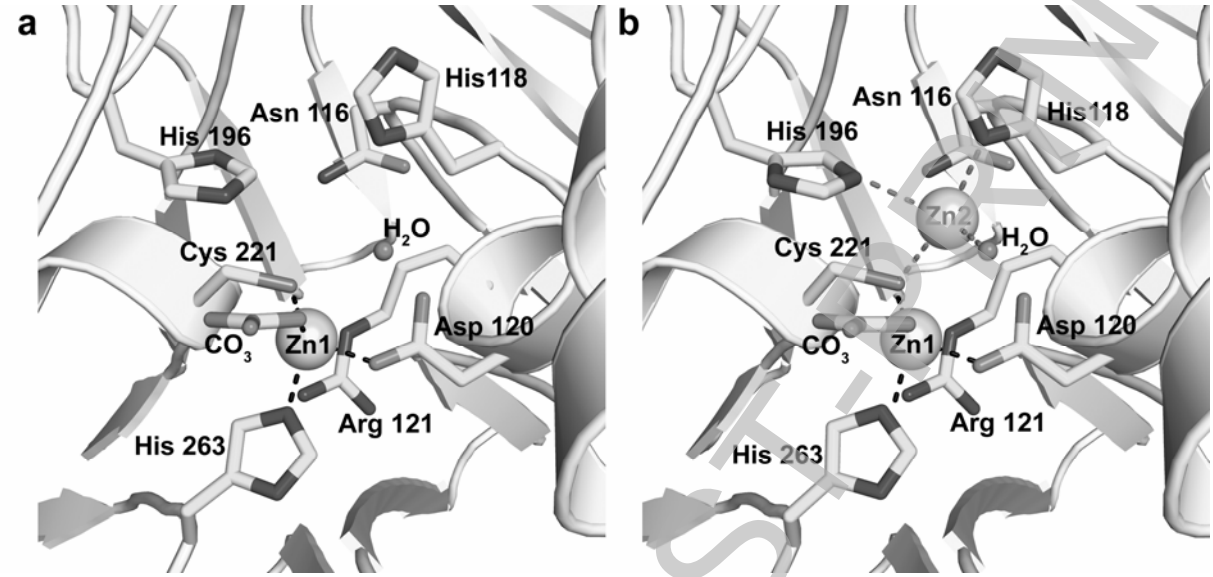

Figure 4 (Bebrone *et al.*)

a)

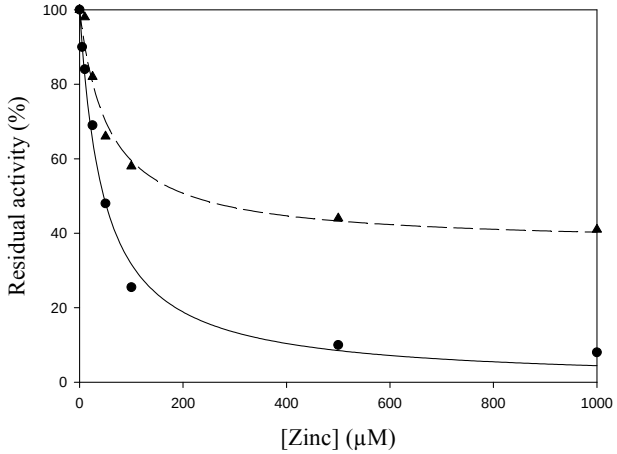

b)